ISME

Experimental Investigation for Wake of the Circular Cylinder by Attaching Different Number of Tripping Wires

A.A. Bakkhoshnevis[*]
Associate Professor

A.R. Mamouri[†]
Ph. D Student

M. Khodadadi[‡]
MSc. Student

An experimental study is conducted on flow past a circular cylinder fitted with some tripping wires on its surface. The work investigates the dependency of the critical wire locations on the wire size and Reynolds numbers, and examines the wake and vortex shedding characteristics in an effort to advance the understanding of the critical wire effects beyond the existing literature. The primary aim of this investigation is to assess the significance of the angular locations of the surface trip wire. For the novelty, 2, 4, 6, 8 and 10 number of trip wires on the circular cylinder surface and for two Reynolds numbers are employed. Furthermore, the two and one tripping wire with 45 and 60 degrees angular positions on the circular cylinder surface that has be found very unstable by the other researchers but, in this study at these two angular positions the unstable relationship is lower by attaching different number of tripping wires on the circular cylinder surface. The cylinders used as test models each had a diameter of 20mm and length of 400mm.

Keywords: Trip wire, Drag coefficient, Strouhal number, Velocity defect, Hot wire.

1 Introduction

External flow around cylindrical or near-cylindrical bodies has been a field of extensive research due to its application in a variety of engineering components or systems for a number of decades but still poses challenging problems. These types of flows are complex even for a simple geometry due to the coexistence of the boundary layer, free shear-layers and a significant region of re circulatory flow.
In classical aerodynamics, these types of bodies are called as blunt bodies or bluff bodies. A traditional example of the bluff body wake flows is encountered around cylinders. In engineering, fluid forces and Strouhal numbers are the major factors considered in the design of multiple slender structures subjected to cross flow, e.g., chimney stacks, tube bundles in heat exchangers, overhead power line bundles, bridge piers, stays, masts, chemical reaction towers

[*] Corresponding Author, Associate Professor, Hakim Sabzevari University, Sabzevar, Iran
khosh1966@yahoo.com
[†] Ph. D Student, Hakim Sabzevari University, Sabzevar, Iran amirelmir3000@yahoo.com
[‡] MSc. Student, Hakim Sabzevari University, Sabzevar, Iran

and skyscrapers. Properties of wake excitation for circular cylinders have been studied by lots of researchers. Wake flow patterns can be controlled by different methods, one can be referred to the Reynolds number effect that worked by Paranthoen [1] and Kuo [2], aspect ratio that worked by Rehimi [3] and Araujo [4], surface roughness that worked by Nagao [5], Aydin [6] and Bragg [7], holding plates dimensions at the end of the cylinder that worked by Wang [8], and blockage. That in these papers, the circular cylinder studied along with the other items. Explanation the issues are not permissible in the recent paper with tripping wires.
In the present paper the effects of surface roughness of the circular cylinder on the control of wake flow were experimentally investigated. This phenomenon causes narrower wake of the circular cylinder, then reducing the total drag coefficient, Khoshnevis has found similar results in this regard, too[9]. Previous research on circular cylinders fitted with some tripping wires on its surface, has shown that the shedding frequency and the mean and turbulence quantities strongly depend on the wires size (fixed at 1.5mm or wire to cylinder diameter ratio is 0.075), wires locations (45˚, 60˚and 36˚, its being defined with respect to the forward stagnation point of the cylinder), number of wires (2, 4, 6, 8, 10, are in the same distances into the cylinder surface) and Reynolds numbers (Re=10000 and Re=35000).

This end, in the present investigation, directly compared the structure of the wake and the separating shear layer for six models (smooth circular cylinder and cylinders with different number of tripping wires on its surface). Most of the previous studies on wakes deal with circular cylinders with tripping wires on its surface. By placing a small cylinder near the main cylinder, Tsutsui [10] controlled streams around the plain cylinder and found that a decrease in the wake width until found the lower drag coefficient.
Hover et al [11] installed two tripping wires on the circular cylinder with low Reynolds number, learned that the installation of a tripping wire on a stable cylinder will significantly decrease lift coefficient, drag force, and increase Strouhal number. Later on, Ekmekci and Rockwell [12] studied the influence of circular cylinder with trip wire on its surface and demonstrated that Strouhal number shows crater-like changes (a gradual decrease and then increase) by changing its angular position across the limits of critical angles. Nishi et al [13], demonstrated that considering the angular position in 20 degrees to 52.5 degrees or more than 97.5 degrees, the forces will decreased, by the tripping wire on the circular cylinder surface. Particularly at 75 degrees angle, the lift and drag coefficient have been increased and at the 112.5 degrees angular position this ratio has been reduced.

Finally, all the previous works were carried out for one, two, three and four trip wires on the circular cylinder surface, while in this work is 2, 4, 6, 8 and 10 number of trip wires on circular cylinder surface and for two Reynolds numbers are employed. It is an extension of the previously obtained results and leads to more experience about this geometry. Then, it was presented the results of mean velocity and turbulence intensity profiles of wake. Furthermore, the results obtained from Alam [14] and Igarashi [15], the two and one tripping wire with 45 and 60 degrees angular positions on the circular cylinder has be found very unstable but, in this study at these two angular positions the unstable relationship is lower by attaching different number of tripping wires on its surface.
In this paper, experimentally studied the Strouhal number and drag coefficient parameters, mean velocity and turbulent intensity profiles of the wake flow patterns at the following stations (X/D) 0, 0.5, 1, 4, 5, 10, 15, 25 and 30, as shown in fig.1b (distance away from the cylinder is X and diameter of the cylinder is D).

2 Methodology

2.1 Experimental set up

Experiments were carried out in a low-speed, open-circuit wind tunnel manufactured by Farasanjesh Saba's company. The test section of the wind tunnel was rectangular with a height of 40cm, width of 40cm and length of 168cm. The cylinder used as test models had a diameter of 20mm and length of 400mm. The velocity in the wind tunnel can be varied from o to 30m/s, using motor speed control.

For all measurements, the free-stream velocity, U_∞; in the tunnel was kept constant at 7.5 m/s and 26 m/s (the Reynolds numbers are 10000 and 35000, respectively). A honeycomb was placed at the entrance of the test section to produce a uniform flow. To corroborate that the flow in the test-section was uniform, a calibrated hotwire installed on two stands, it was traversed across the whole test section of the tunnel. Diameter of the hot wire is 0.0005 micrometer. It is manufactured from tangsten. In the same region, the turbulence intensity was also uniform and less than 0.1% of the free-stream velocity. The schematic diagram of the wind tunnel and the symmetrical arrangement of two tripping wires (for example) on the circular cylinder surface and the coordinate system are shown in Figure (1).
The wind tunnel used in this experiment and the model arrangement of 8 tripping wires (for example) on the circular cylinder surface are shown in Figure (2). Flow measurements were conducted with constant temperature anemometry (CTA) technique to obtain information of the flow around the circular cylinder with and without tripping wires. (The output voltage of hot wire anemometer is dependent on the rate of hot wire sensor heat transfer to the fluid. Therefore, the temperature difference between the hot wire sensor and the fluid flow assumed constant for measuring the fluid flow velocity.)
The anemometer of constant temperature hot wire is able to measure mean velocity, turbulence intensities and vortex shedding frequency. The experiments accomplished through a one dimensional probe that having a sensor with 1.25mm length and 5μm diameter. Each test model considered a circular cylinder (which is made of Plexiglass), on the outer surface of which, parallel to its span, number of tripping wires was tightly stretched and glued. The plain circular cylinder had a diameter of 20mm and length of 400mm, and the surface trip wires had diameter of 1.5mm.

Thereby, during the course of investigation, consideration was given to six separate test models, the smooth circular cylinder and the cylinder which had different number of tripping wires (2, 4, 6, 8 and 10, respectively) with wire_ to_ cylinder diameter ratio of 0.075.
Experiments were carried out at two different Reynolds numbers, Re=10000 and Re=35000 (based on the circular cylinder diameter D). To explore the significance of the number of wires and the wire angular location, the trip wire was positioned at varying angular locations based on the number of trip wires on the circular cylinder surface in 45˚, 60˚ and 36˚, that are in the same distance from each other (these angles defined with respect to the forward stagnation point of the circular cylinder).
In order to run these experiments, at first, the smooth circular cylinder was placed inside the settling chamber. Then the cylinder with 2, 4, 6, 8 and 10 tripping wires on its surface placed inside the settling chamber, respectively.

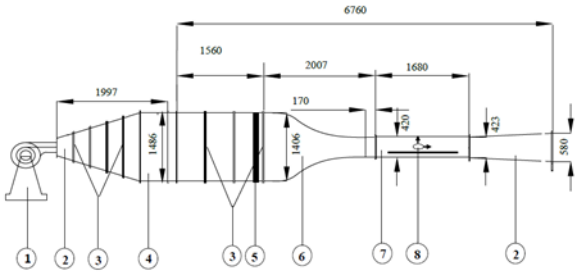

(a)

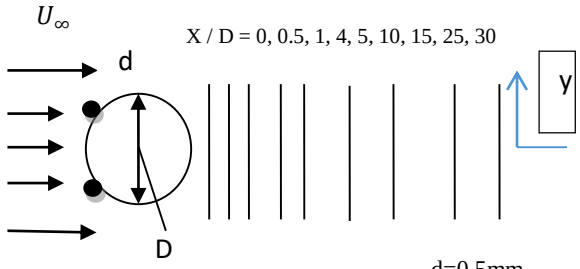

(b)

Figure 1 schematic diagram of a) the wind tunnel: 1. Centrifugal blower, 2. Diffuser, 3. Nylon screen, 4. Settling chamber 5. Honey comb, 6. Contraction, 7. Test section, 8. Circular cylinder, b) the model used (with two trip wires) (diameter of wires is d and stations away from the cylinder are x/D)

(a)

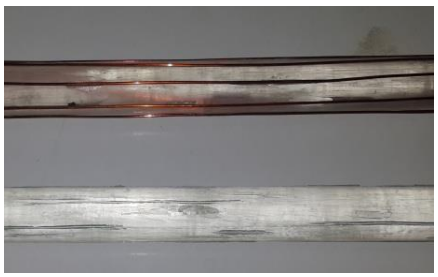

(b)

Figure 2 a) The wind tunnel used in this experiment, b) the model with 8 tripping wire on the circular cylinder surface

2.2 Velocity defect, half width and turbulence intensity parameters

Wake is classified as a thin shear layer within which rapid variations of flow variables such as velocity and turbulence intensities take place. The velocity in the wake is smaller than that in the free stream and therefore a so_ called velocity defect (W_0) exists. As the free stream

distance increases, due to the wake, the differences between velocities become smaller and smaller. At any cross section of the wake, the velocity drops from the free stream value, first gradually and then sharply to a minimum value on the centerline, where the maximum velocity defect occurs. At the other hand, the width wake in the mean velocity profiles is found to be, inversely related with the velocity defect that is so_ called half width ($b_{½}$). The velocity defect and half width parameters has shown in Figure (3).

Velocity defect and turbulence intensity parameters can be calculated by the following equations:

$$\frac{W_{\circ}}{U_{\infty}} = \frac{U_{\infty} - U_{min}}{U_{\infty}} \quad (1)$$

That U_{min} is the minimum velocity and the U_{∞} is the free stream velocity in this equation.
The turbulence intensity parameter is defined in equation 2. That U' is one component of turbulence intensities.

$$TU\% = \frac{\sqrt{\overline{U'^2}}}{U_{\infty}} \times 100 \quad (2)$$

Half width parameter can be measured in the figure 3. In the results presented in this paper, the mean velocity and turbulence intensity profiles are normalized with respect to the mainstream velocity U_{∞} (U_{ref}).

2.3 The Struohal number and drag coefficient (by wake_ survey method)

The vortex_ shedding frequency, when normalized with the free stream velocity U_{∞} (U_{ref}) and the circular cylinder diameter D, can on dimensional grounds be seen to be a function of the Reynolds number:

$$St = St(Re) \quad (3)$$

In which;

$$St = \frac{fD}{U_{\infty}} \quad (4)$$

And "f" is the vortex _shedding frequency. The normalized vortex _shedding frequency, namely St, is called the Strouhal number.
Vandom [17] was obtained the equation to calculation the drag coefficient. There was the Reynolds stress terms and flow turbulence intensities terms in this equation, whereas, flow density variations

and viscous term $\mu \frac{\partial U}{\partial y}$ there were not in this equation [16, 17]. In generally, this equation is as below:

$$C_d = \int \left(\frac{p_{s,e} - p_{s,w}}{q_{\infty}}\right) d\left(\frac{y}{l}\right) + 2\int \frac{\overline{u}}{U_{\infty}}\left(1 - \frac{\overline{u}}{U_{\infty}}\right) d\left(\frac{y}{l}\right) - 2\int \frac{\overline{U'^2}}{U_{\infty}}\, d\left(\frac{y}{l}\right) \quad (4)$$

The two integrals in the last, related to the turbulence intensities. This equation is composed in three parts:

1) The pressure term:

$$\int \left(\frac{P_{s,e} - P_{s,w}}{q_{\infty}}\right) d\left(\frac{y}{l}\right) \quad (5)$$

2) The momentum term:

$$2\int \frac{\overline{U}}{U_{\infty}}\left(1 - \frac{\overline{U}}{U_{\infty}}\right) d\left(\frac{y}{l}\right) \quad (6)$$

3) The Reynolds stress term:

$$2\int \frac{\overline{U'^2}}{U_{\infty}} d\left(\frac{y}{l}\right) \quad (7)$$

Therefore, According to Goldstein analysis [18]:

$$P_{s,e} = P_{s,w} + \bar{q}' \tag{8}$$

$$\bar{q}' = \frac{1}{2}\rho\left(\overline{u'^2} + \overline{v'^2} + \overline{w'^2}\right) \tag{9}$$

By substituting the parameters in the original equation;

$$C_d = 2\int \sqrt{\frac{q}{q_\infty}}\left[1 - \sqrt{\frac{q}{\infty}}\right] d\left(\frac{y}{l}\right) + \left[\int \sqrt{\frac{(\overline{u}'^2+\overline{v}'^2-\overline{w}'^2)}{{U_\infty}^2}}\right] d\left(\frac{y}{l}\right) \tag{10}$$

In this equation, assuming the components of turbulence intensities (u´=v´=w´) are homogeneous, in the last stations (far wake from the cylinder), and some of the mean velocity terms as $\bar{v}$ and $\bar{w}$ are very tiny according to the vandom's equation and these terms can be neglected.

$$C_d = 2\int \sqrt{\frac{q}{q_\infty}}\left[1 - \sqrt{\frac{q}{q_\infty}}\right] d\left[\frac{y}{l}\right] + \int \left[\frac{q'}{q_\infty}\right] d\left[\frac{y}{l}\right] \tag{11}$$

3 Validation

The mean velocity profiles for the smooth surface circular cylinder are validated with the karamanos [19] mean velocity profiles, in the same stations$\frac{x}{d} = 5$. Both of two experiments are at Incompressible flow and low Reynolds numbers (Reynolds numbers are less than 50000). As shown in Figure (4), the mean velocity profile is validated by karamanos work (the smooth circular cylinder).

The Strouhal number for the smooth surface circular cylinder is validated with that of the other Researchers in table1.

Values are about the same, and the very small difference between them caused by the environmental conditions and accuracy of measurement devices.

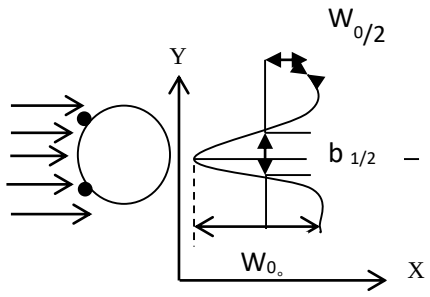

Figure 3 Velocity defect and half width parameters

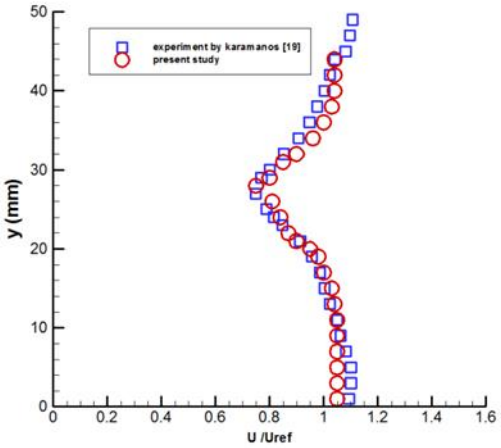

Figure 4 diagram of mean velocity validated by Karamanos [19] for the smooth surface circular cylinder

Table1 Strouhal number validated by the other researchers, for smooth circular cylinder

	Strouhal number
In this paper	0.188
Alem [6]	0.2
Hover [6]	0.185
Sakamoto [14]	0.19

4 Results and discussions

4.1 Smooth circular cylinder

Normalized diagrams of mean velocity and turbulence intensity profiles versus the sampling interval have been plotted for all stations for the smooth surface circular cylinder in flowing figures. The results show the formation of asymmetric wake about the wake centerline, and a distinguishing feature of these profiles is the existence of a double peak (in Re=35000 are more than Re=10000).

Figure (5c) (mean velocity profile at Re=35000) clearly shows that, as the free stream distance from the cylinder increases, both peaks move away from the wake centerline and the profiles become flatter, at station x/d=4. It should be noted that, indicates bigger vortices, duo to the double peak, and so on, as the free stream distance from the cylinder increases, the bigger vortices convert to eddy. Whereas, in Figure (5a) (mean velocity profile at Re=10000) approximately, does not recognized the double peak in the near wake of the cylinder, due to minimum velocity in the near wake.

As the free stream distance from the cylinder increases, the differences between the free stream velocity and wake velocity, becomes smaller and smaller, and it causes diminishing of the bigger vortices inside the wake of the cylinder. By increasing free stream distances, velocity defect decreased following the stations.

In the other hand, as shown in Figures (5a and 5c), distinct the existence of a double peak in the near wake (at stations: 0 and 0.5).

This phenomenon is duo to the vortex shedding frequency in the wake of the cylinder. At any cross_ section of the wake, the pressure drops, sharply on the centerline, where the maximum velocity occurs, because of the vortex shedding. So, this drop pressure in cylinder with bigger Reynolds number (Re=35000) is more than that one by smaller Reynolds number (Re=10000).

The next differences between 5a and 5c (mean velocity profiles in two Reynolds numbers), are in wake width and velocity defect.

The velocity defect in mean velocity profiles at Re = 35000 is more than that at Re =10000, also, wake width for the case at Re = 35000 is smaller than that at Re = 10000. In addition, it was found in Figures (5a and 5c), all of the points outside the wake, nearly progress to the same value. That means the experimental carried out for the same conditions. The intersection point explains sites of vortex shedding formation in the wake of the cylinder. As shown in (Figures 5b and 5d), the maximum turbulence intensity peaks are seen in the same points with mentioned earlier about intersection points (Figures 5a, 5c).

In this Figures (5b, 5d), was shown minimum turbulence intensities in the wake centerline, duo to, the small vortices in the wake centerline and existence of reverse flow in there.

A distinguishing feature of these profiles is the existence of a double peak, as the free stream distance from the cylinder increases, both peaks move away from the wake centerline and the profiles become flatter. Although, as the free stream distance from the cylinder increases, turbulence intensity profiles reach to the 10% ratio (it was quickly in case at Re=35000). It can be said, in case at Re=35000, turbulence intensity peaks are maximum, but the maximum wake width of turbulence intensity profiles is relevant to the case at Re = 10000.

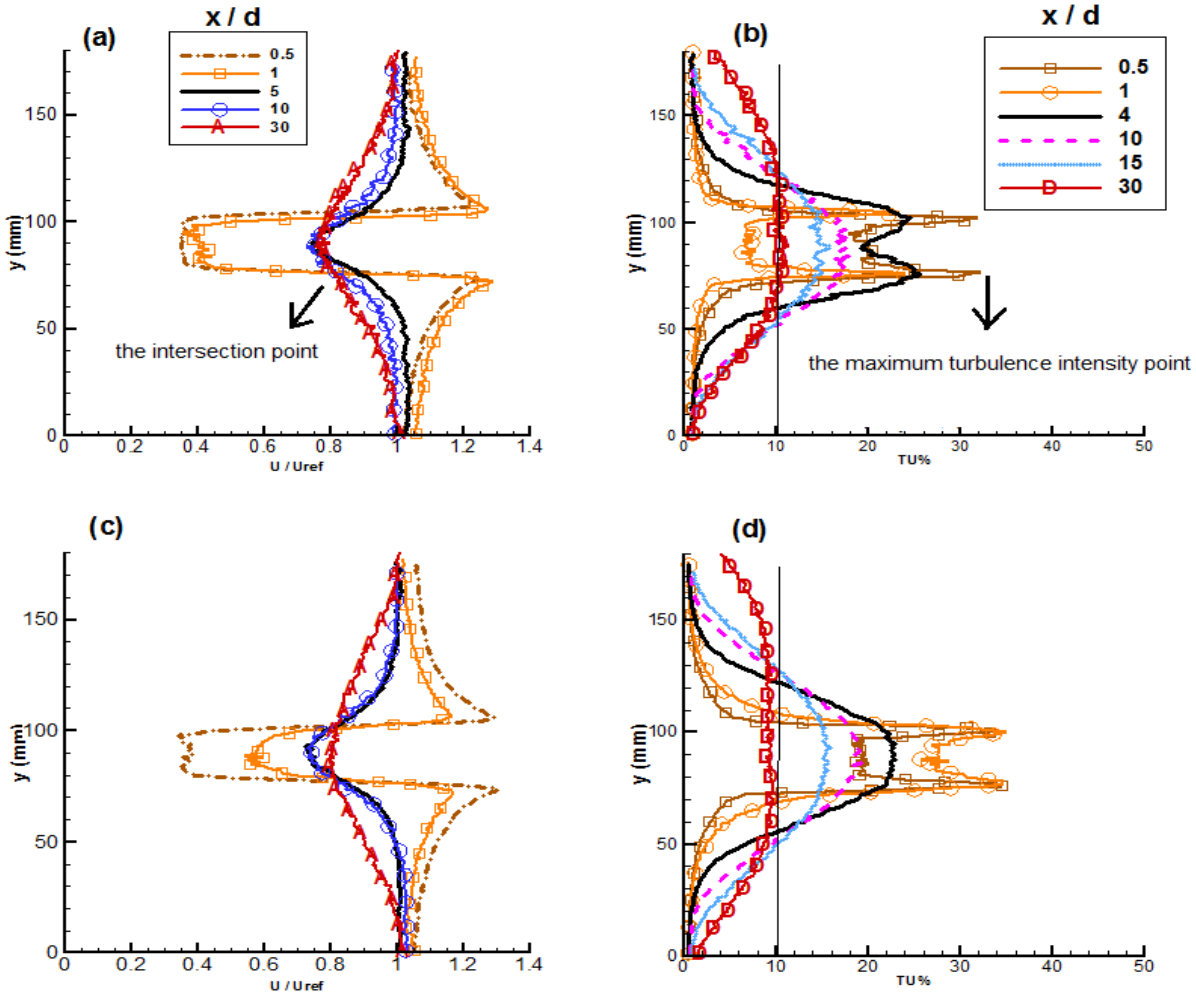

Figure 5 Normalized diagrams of a) mean velocity profile and b) turbulence intensity profile at Re = 10000, and Normalized diagrams of c) mean velocity profile and d) turbulence intensity profile at Re = 35000, versus the sampling interval for the smooth circular cylinder in all of the stations

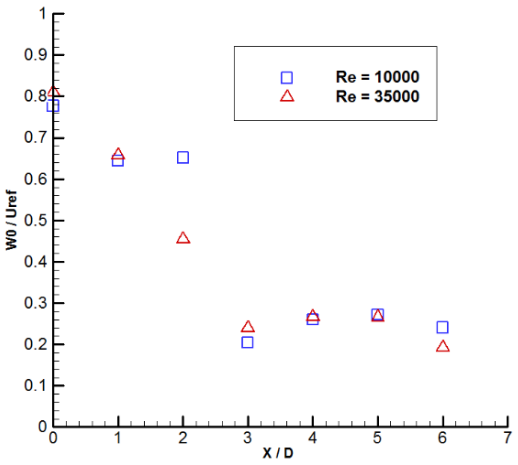

Figure 6 Velocity defect in all of the stations for smooth surface circular cylinder in two Reynolds number

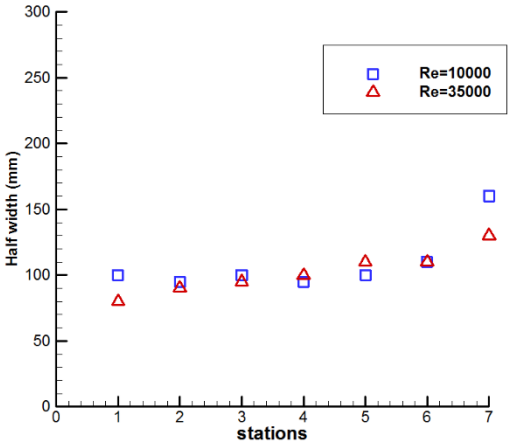

Figure 7 half width in all of the stations for smooth surface circular cylinder in two Reynolds number

The velocity defect profiles are shown in Figure (6). Therefore, the velocity defect in tests for circular cylinder at Re=35000 is more than that at Re=10000, over the most of stations. In the last stations (far wake from the cylinder), velocity defect for the case at Re=35000 reduced, more quickly. It is a large difference of velocity defects in x/D=2, that is because of that, the station is very near the cylinder, and the turbulence intensities in this station are maximum.
The half width profiles in successive stations are shown in Figure (7). Therefore, the half width in tests for circular cylinder at Re=35000 is less than that at Re=10000, over the most of stations. In the last stations (far wake from the cylinder), half width for the case at Re=10000 increased, more quickly. Therefore, it was shown in Figures (7 and 8) that the velocity defect is found to be, inversely related with width wake.

4.2 mean velocity

The mean velocity variations profiles and turbulence intensity variations profiles versus the number of tripping wires (0, 2, 4, 6, 8 and 10, respectively) in wire_ to_ cylinder diameter d/D=0.075, on a circular cylinder surface in successive stations are shown in Figures (8), (9), (10) and (11) (in two Reynolds numbers). As it can be seen in Figure (8) (Re=35000), wake of the cylinder became wider, by decreasing the number of tripping wires on circular cylinder surface. In other words, as the shear layer magnitude decreased ($\frac{dU}{dy}$ decreased), the velocity

defect has been lowered. Of course, it has be seen, the wake width and velocity defect are the same for the cylinder with 4 and 8 trip wires on its surface (45˚), nearly.
It can be said even that the wake width is narrower for the cylinder with 4 and 8 trip wires on its surface, and the velocity defect is maximum in these models. Then, the velocity defect decreased and wake width increased, reversely, by decreasing tripping wires on the circular cylinder surface (10, 6 and 2, respectively). In circular cylinder with 6 trip wires on its surface, the double peak behind the cylinder is maximal, whereas, at the other models is the same amount, almost (both peaks are maximum in the smooth circular cylinder). In general it can be said, drop pressure decreased on the wake of the cylinder by increasing tripping wire on the cylinder surface (cylinder with 6 trip wires on its surface is distinct). The larger vortices behind the smooth circular cylinder and cylinder with 6 trip wires on its surface are more than that of the other models. Moreover, as increasing the distance of free stream, all the diagrams end are at the same range of mean velocity (similar to the smooth cylinder), it can be seen in Figure (9) (Re =10000), too.

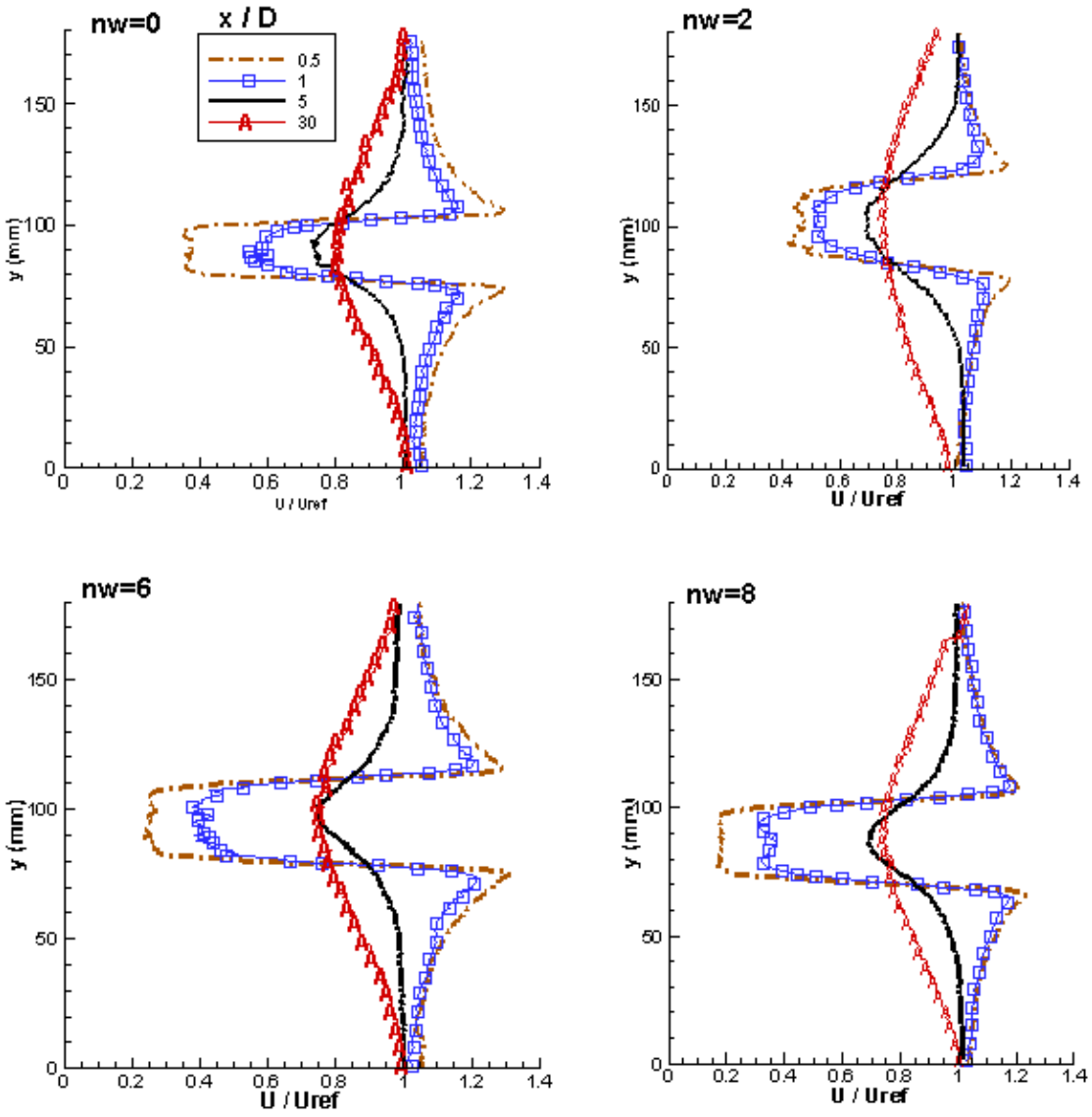

Figure 8 Normalized diagrams of mean velocity profiles in Re=35000 versus the sampling interval for the circular cylinder with different number of trip wires on its surface ($\frac{d}{D}$ =0.075) in all stations (nw is the number of wire sign)

As shown in Figure (9), for the cylinder with 4 tripping wires on its surface the wake width is narrower, whereas, the velocity defect is maximal. Then, the velocity defect decreased and wake width increased by decreasing the number of tripping wires on the circular cylinder surface (10, 8, 6 and 2, respectively). The smooth circular cylinder behavior is between the cylinders with 8 and 6 trip wires on its surface.
According to these results, in both Reynolds numbers behavioral similarities can be seen, for all models. According to the above, it can be seen a lot of Instability for the cylinder with 2 trip wires on its surface. In general, it can be said, the velocity defect in models at Re =35000 is more than that of at Re =10000. of course, wake width in models at Re =35000 is narrowest and Can be allocated to lower drag coefficients.

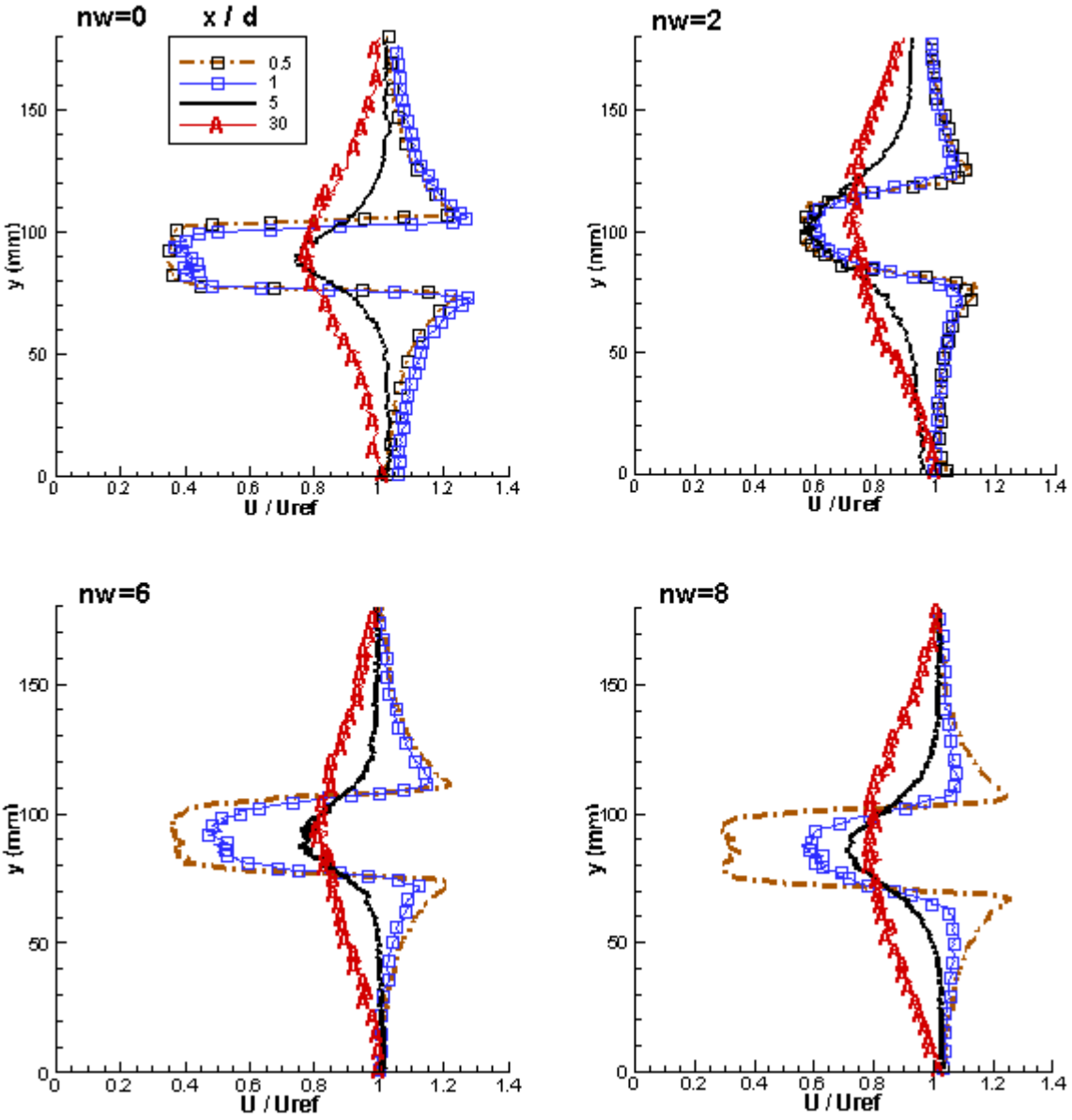

Figure 9 Normalized diagrams of mean velocity profiles in Re=10000 versus the sampling interval for the circular cylinder with different number of trip wires on its surface ($\frac{d}{D}$ =0.075) in all stations (nw is the number of wire sign)

4.3 turbulence intensity

The following plots of turbulence intensities are shown in Figures (10) and (11), for two Reynolds numbers. The results presented below (Figure (10)), the maximum turbulence peaks for the circular cylinder with 4 and 8 tripping wires on its surface is less than that of the other models, while, the wake width of turbulence intensity in these two models is more than that of the other models.
Also, the maximum turbulence intensity peaks for the circular cylinder with 2 trip wires on its surface is more than that of the other models, whereas, the wake width of turbulence intensity in this model is less than that of the other models.

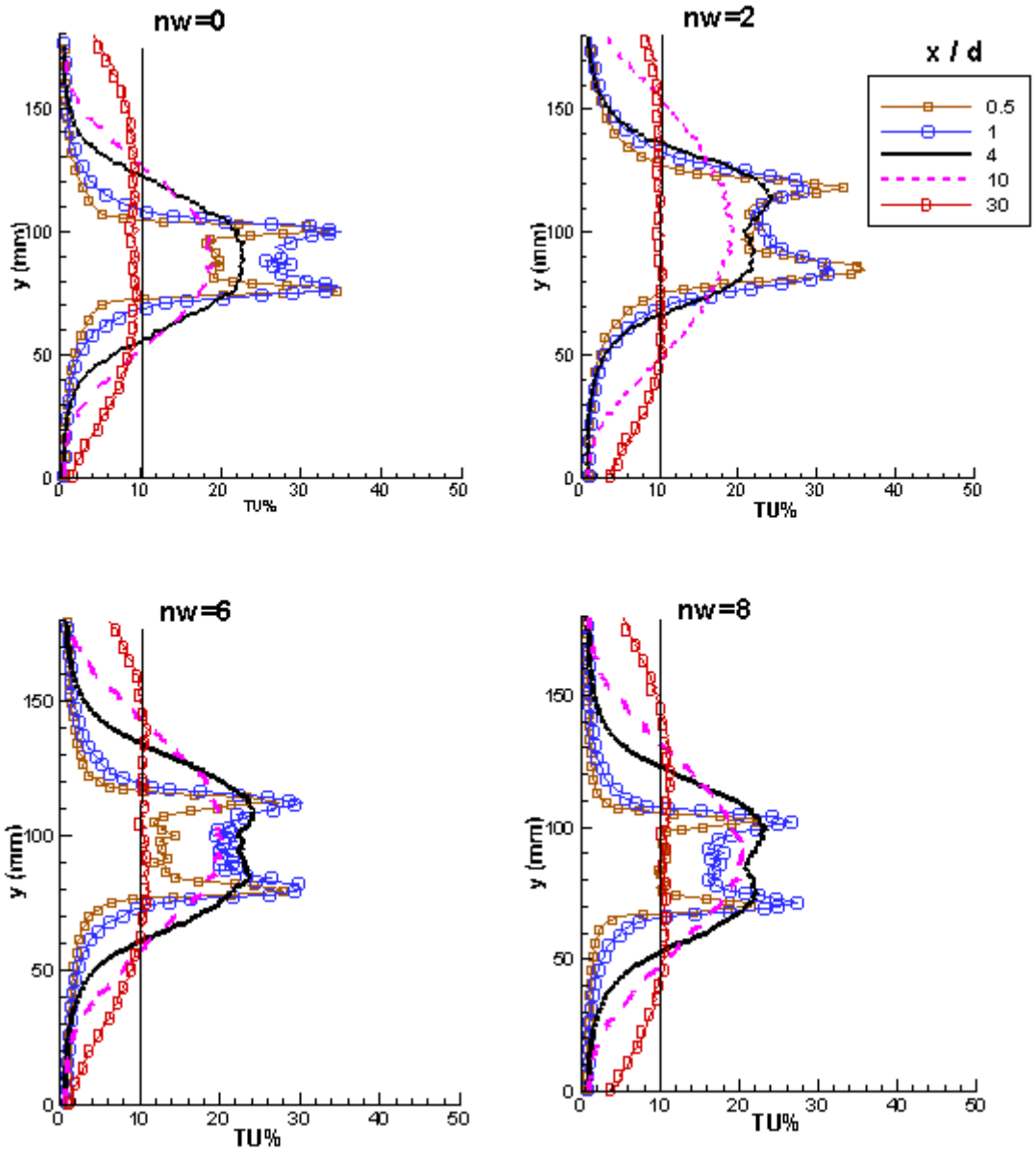

Figure 10 Normalized diagrams of turbulence intensity profiles in Re=35000 versus the sampling interval for the circular cylinder with different number of trip wires on its surface ($\frac{d}{D}$ =0.075) in all stations (nw is the number of wire sign)

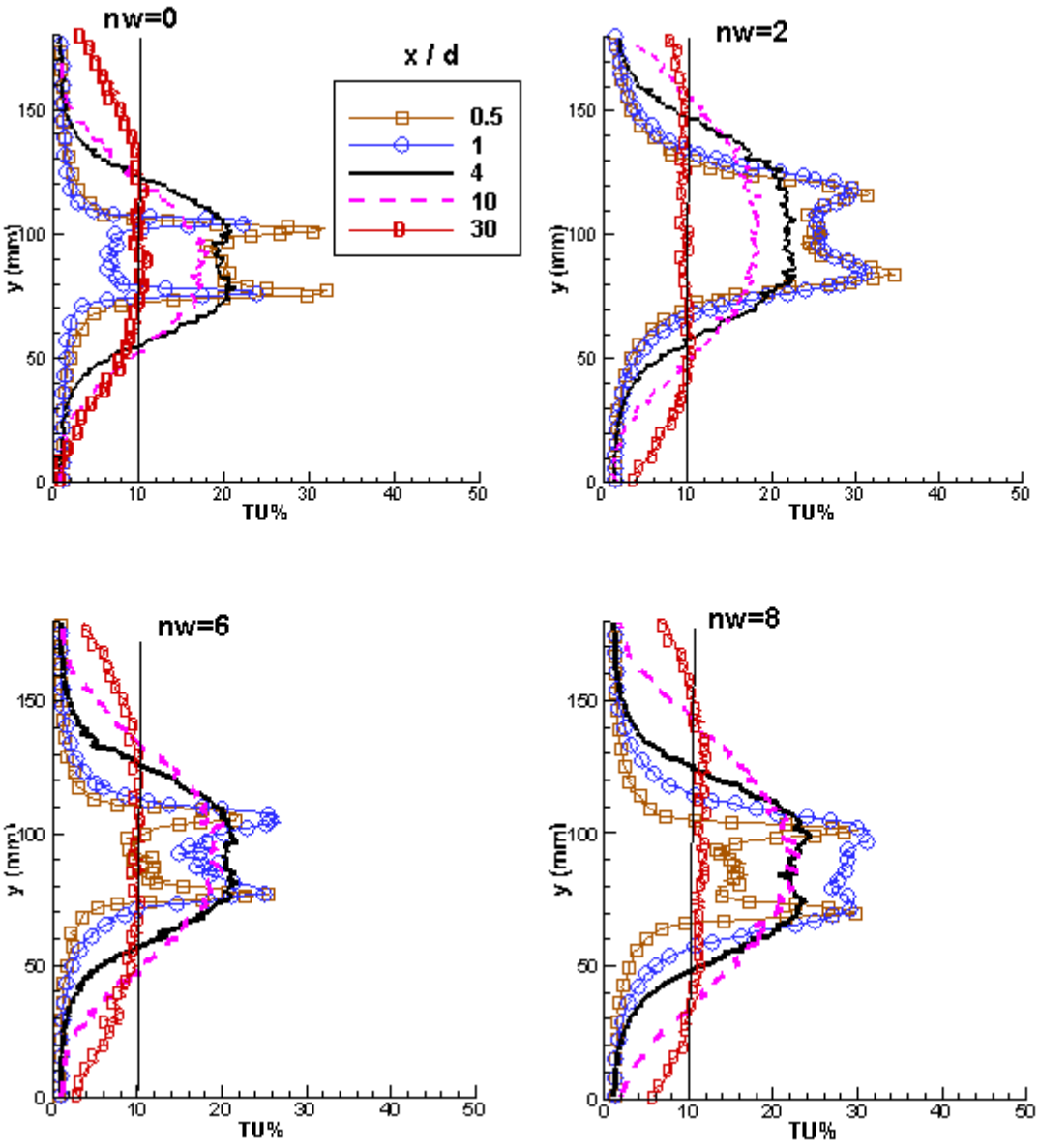

Figure 11 Normalized diagrams of turbulence intensity profiles in Re=10000 versus the sampling interval for the circular cylinder with different number of trip wires on its surface ($\frac{d}{D}$ =0.075) in all stations (nw is the number of wire sign)

In other words, the trend in the wake width of turbulence intensity variation is opposite to that of the maximum turbulence intensity peaks with change in number of tripping wires (or angular position of tripping wires on the cylinder surface). As previously noted (Figure (5)), the maximum turbulence intensity peaks are due to the center of vortex shedding in wake of the circular cylinder.

The turbulence intensity profiles at Re=10000, are shown in Figure (11). As shown in these profiles, the turbulence intensity peaks for the circular cylinder with 2 trip wires on its surface are maximal and these are minimal for the cylinder with 6 and 4 trip wires on its surface.

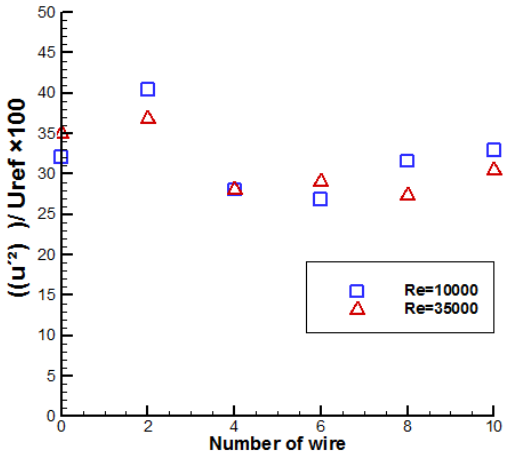

Figure 12 plots of the maximum turbulence intensity, for the smooth circular cylinder and the cylinder with different number of tripping wires on its surface ($\frac{d}{D}$ =0.075), for two Reynolds numbers

The turbulence intensity peaks for the smooth circular cylinder and the cylinder with 10, 8 and 4 tripping wires on its surface are between the cylinders with 2 and 6 trip wires on its surface. According to these profiles in Figures (10) and (11), the maximum turbulence intensity peaks are seen in the same points with mentioned earlier about intersection points in Figures (8) and (9). Although, as the free stream distance from the cylinder increases, turbulence intensity profiles reach to the 10% ratio (it was quickly in case at Re=35000). It can be said, in models at Re=35000, turbulence intensity peaks are maximum, but the maximum wake width of turbulence intensity profiles is relevant to the models at Re = 10000.

The maximum turbulence intensity plots are shown in Figure (12). In other words, it can be verified the results of the other plots in Figures (8), (9), (10) and (11). In Figure (12), the highest maximum turbulence intensity peaks (in stations near the cylinder) are related to the models at Re=35000. As previously noted, the turbulence intensity peaks for the cylinder with 4 and 6 tripping wires on its surface are minimum, at Re=10000, whereas, the turbulence intensity peaks for the cylinder with 4 and 8 tripping wires on its surface are minimum, at Re=35000.

4.4 velocity defect & half width

For more explanation, velocity defect diagrams in all of the stations and in two Reynolds numbers has been shown in Figure (13). As shown in Figure (13), the velocity defect for circular cylinders with 4 and 8 trip wires on its surface in all of the stations, almost, is more than that of the other models in both Reynolds numbers, and the velocity defect is minimal for cylinder with 2 trip wires on its surface. Also, it can be said, the velocity defect gradient in smooth circular cylinder is more than that of the other models, whereas, the velocity defect gradients are the mostly same for the cylinders with tripping wires on its surface. However, the velocity defect gradient in cylinder with 2 tripping wires on its surface is at least. Then, the half width diagrams in all of the stations and in two Reynolds numbers has been shown in Figure (14). As shown in Figure (14), the wake width for the smooth circular cylinders in all of the stations, almost, is less than that of the other models in both Reynolds numbers. The wake width for circular cylinders with 2 and 10 trip wires on its surface in all of the stations, almost, is more than that of the other models and for the cylinder with 6, 4 and 8 trip wires on its surface it is less than

that the other models, in Re=10000. These conditions are true in Re = 35000, too, but the wake width in cylinder with 6 trip wire on its surface increased.
Also, it can be said, the wake width gradient in smooth circular cylinder is less than that of the other models, whereas, the wake width gradients are the mostly same for the cylinders with tripping wires on its surface. Duo to the Figures (13) and (14), the maximum velocity defect is found to be, inversely related with the wake width. The velocity defect plots are shown in Figure (15). In other words, it can be verified the results of the other plots in Figures (8), (9), (10) and (11). In Figure (15), the highest velocity defect peaks (in stations near the cylinder) are related to the models at Re=35000, mostly.
As previously noted, the velocity defect for the cylinder with 4 trip wires on its surface is more than that of the other models, whereas, the velocity defect for the cylinders with 4 and 8 trip wires on its surface is more than that of the other models, at Re=35000. As can be seen in this figure and Figure (12), the trend in velocity defect variation is opposite to that of the turbulence intensity peaks with change in the number of tripping wires.

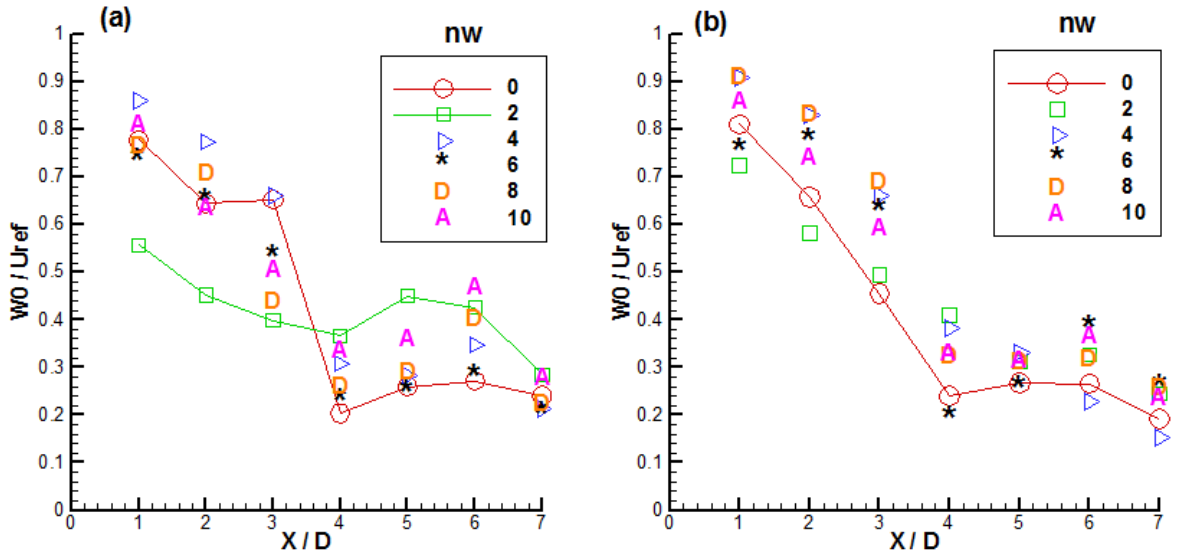

Figure 13 the velocity defect diagrams for all of the stations (X/D), a) Re =10000, b) Re =35000 (d/D=0.075)

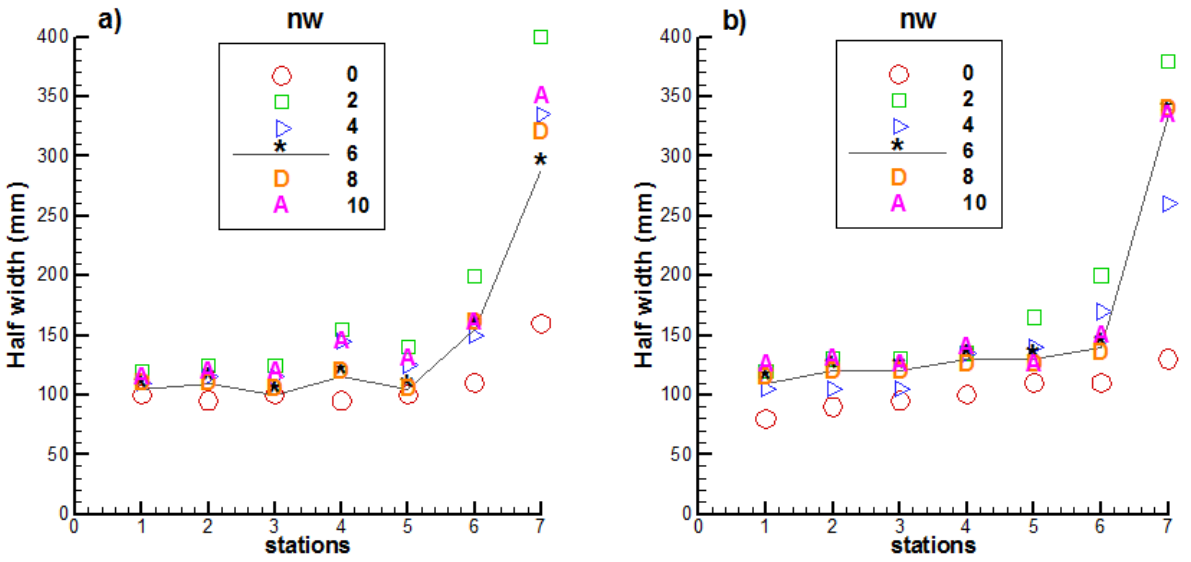

Figure 14 the half width diagrams for all of the stations (X/D), a) Re =10000, b) Re =35000 (d/D=0.075)

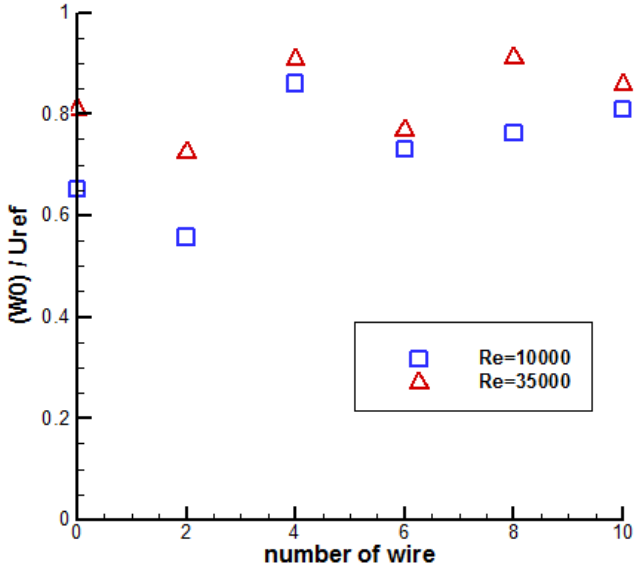

Figure 15 plots of the velocity defect, for the smooth circular cylinder and the cylinder with different number of tripping wires on its surface ($\frac{d}{D}$ =0.075), for two Reynolds numbers

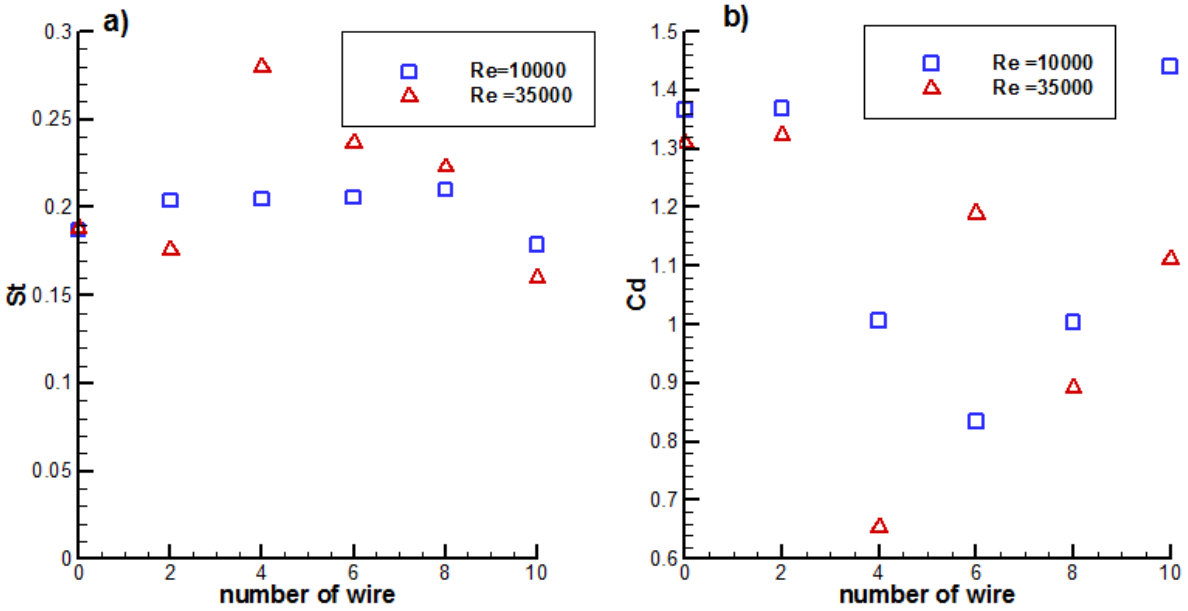

Figure 16 plots of a) the Strouhal number and b) drag coefficient, for the smooth circular cylinder and the cylinder with different number of tripping wires on its surface ($\frac{d}{D}$ =0.075), for two Reynolds numbers

4.5 strouhal number & drag coefficient

Finally, the Strouhal number plots and the drag coefficient plots are shown in Figure (16), in both of tow Reynolds numbers. As shown in this figure, the trend in Strouhal number variation is opposite to that of the drag coefficient (Hover [11] obtained similar results), with change in the number of tripping wires on the cylinder surface.

In general, drag coefficient decreased and the Strouhal number increased, by increasing the number of tripping wires on the circular cylinder surface. Drag coefficient in models at Re=35000 is less than that of the models at Re=10000, and so on, the effects of tripping wires on the cylinder surface at Re=35000 are more visible. As shown in Figure (16), the Strouhal number shows crater-like changes (a gradual decrease and then increase) by changing its angular position across the limits of critical angles by different number of the tripping wires on the cylinder surface, as Ekmekci [12] obtained these results by different angular positions of the tripping wires on the cylinder surface. In both of two Reynolds numbers the Strouhal number magnitude is equal, nearly.

5 Conclusion

An experimental study is conducted on flow past a circular cylinder fitted with some tripping wires on its surface. The work investigates the dependency of the critical wire locations on the wire size and Reynolds numbers, and examines the wake and vortex shedding characteristics in an effort to advance the understanding of the critical wire effects beyond the existing literature. The primary aim of this investigation is to assess the significance of the angular locations of the surface trip wire. The wire size is 1.5 mm (wire_ to_ cylinder diameter ratio is 0.075), where in different angular locations attached in to the cylinder (by different number of trip wires, 2, 4, 6, 8, 10) and two Reynolds numbers (Re=10000 and Re=35000)
In generally, the results it can be listed as below:

- The tripping wires positioning at 45˚ (with 4 trip wires) maximally decreased the drag coefficients by 53% and 65.5% (Re=10000 and Re=35000, respectively), in comparison with the coefficients produced without the tripping wires.
- The variations of the Strouhal number is found to be, roughly, inversely related with drag coefficient, and the drag coefficient reduction for the models at Re=35000 is more than that of the models at Re=10000.
- The maximum velocity defect is the value at the wake centerline is found to be, inversely related with maximum turbulence intensity peaks and width wake, whereas, it is found to be, directly related with shear layer.
- The velocity defect for the circular cylinder with 4 and 8 tripping wires on its surface is maximal, whereas, it is minimal for the cylinder with 2 tripping wires on its surface.
- The instability on the circular cylinder with 6 trip wires on its surface (with 60 degrees angular position) in Re = 10000 is less than that this on Re = 35000 and it is less than that the other researchers studies.

References

[1] Paranthoën, P., and Browne, L. B., "Characteristics of the Near Wake of a Cylinder at Low Reynolds Numbers", European Journal of Mechanics - B/Fluids, Vol. 18, No. 4, pp. 659–674, (1999).

[2] Kuo, C. H., Chiou, L. C., and Chen, C. C., "Wake Flow Pattern Modified by Small Control Cylinders at Low Reynolds Number", Journal of Fluids and Structures, Vol. 23, No. 6, pp. 938–956, (2007).

[3] Rehimi, F., Aloui, F., Nasrallah, S. B., Doubliez, L., and Legrand, J., "Experimental Investigation of a Confined Flow Downstream of a Circular Cylinder Centered between Two Parallel Walls", Journal of Fluids and Structures, Vol. 24, No. 6, pp. 855–882, (2008).

[4] Araújo, T. B., Sicot, C., Boree, J., and Martinuzzi, R. J., "Influence of Obstacle Aspect Ratio on Tripped Cylinder Wakes", International Journal of Heat and Fluid Flow, Vol. 35, pp. 109–118, (2012).

[5] Nagao, F., Noda, M., Inoue, M., and Matsukawa, S., "Propertice of Wake Excitation in Tandem Circular Cylinders with Several Kinds of Surface Roughness", the Seventh International Colloquium on Bluff Body Aerodynamics and Applications (BBAA7), Shanghai, China, (2012).

[6] Aydin, T. B., Joshi, A., and Ekmekci, A., "Critical Effects of a Spanwise Surface Wire on Flow Past a Circular Cylinder and the Significance of the Wire Size and Reynolds Number", Journal of Fluids and Structures, Vol. 51, pp. 132–147, (2014).

[7] Diebold, J. M., and Bragg, M. B., "Study of a Swept Wing with Leading-edge Ice using a Wake Survey Technique", 51st AIAA Aerospace Sciences Meeting, Texas, (2013).

[8] Wang, X. K., and Tan, S. K., "Comparison of Flow Patterns in the Near Wake of a Circular Cylinder and a Square Cylinder Placed Near a Plane Wall", Ocean Engineering, Vol. 35, No. 5-6, pp. 458–472, (2008).

[9] Khoshnevis, A. B., Vahidi, M., and Pedram, M., "Experimental Study for Drag Reduction about Circular Cylinder by Ataching Trip Wire", J. Fluid Dynamics, Vol. 2, No. 2, (2011). (in Persian)

[10] Igarishi, T., and Tsutsui, T., "Flow Control around a Circular Cylinder by a Small Cylinder", 11th Australasian Fluid Mechanics Conference, University of Tasmania, Hobart, Australia, (1992).

[11] Hover, F. S., Tvedt, H., and Triantafyllou, M. S., "Vortex-induced Vibrations of a Cylinder with Tripping Wires", Journal of Fluid Mechanics, Vol. 448, pp. 175-195, (2001).

[12] Ekmekci, A., and Rockwell, D., "Control of Flow Past a Circular Cylinder Via a Spanwise Surface Wire: Effect of the Wire Scale", Experiments in Fluids, Vol. 51, No. 3, pp. 753-769, (2011).

[13] Quadrante, L. A. R., and Nishi, Y., "Amplification/Suppression of Flow-induced Motions of an Elastically Mounted Circular Cylinder by Attaching Tripping Wires", Journal of Fluids and Structures, Vol. 48, pp. 93–102, (2014).

[14] Alam, M. M., Sakamoto, H., and Moriya, M., "Reduction of Fluid Forces Acting on a Single Circular Cylinder and Two Circular Cylinders by using Tripping Rods", Journal of Fluids and Structures, Vol. 18, No. 3-4, pp. 347–366, (2003).

[15] Igarishi, T., "Effect of the Tripping Wires on the Flow around a Circular Cylinder Normal to an Airstream, Bulletin of JSME, Vol. 29 No. 255, pp. 2917-2924, (1986).

[16] Lu, B., and Bragg, M. B., "Experimental Investigation of the Wake-survey Method for a Bluff Body with a Highly Turbulent Wake, 20th AIAA Applied Aerodynamics Conference, Missouri, (2002).

[17] Dam, C. P. V., "Recent Experience with Different Methods of Drag Prediction", Progress in Aerospace Sciences, Vol. 35, No. 8, pp. 751-798, (1999).

[18] Goldstein, S., "A Note on the Measurement of Total Head and Static Pressure in a Turbulent Stream", Proceedings of the Royal Society a Mathematical, Physical and Engineering Sciences, Vol. 155, No. 886, pp. 570-575 , (1936).

[19] Ma, X., Karamanos, G. S., and Karniadakis, G. E., "Dynamics and Low-dimensionality of a Turbulent near Wake", Journal of Fluid Mechanics, Vol. 410, pp. 29–65, (2000).

Nomenclature

C_d	Drag coefficient
D	Diameter of circular cylinder (mm)
f	Vortex shedding frequency
N w	Number of wire
P_s	Static pressure (N/m²)
q	Dynamic pressure (N/m²)
St	Strouhal number
Tu	Turbulence intensity
U	Velocity (m/s)
$\bar{U}$	Mean velocity (m/s)
u', v', w'	Turbulence intensity components
W_0	Velocity defect

Greek signs

μ	Dynamic viscosity (Ns/m²)
ρ	Density (Ns/m²)

Subtitles

∞(ref)	Free stream
e	Value at the edge of the wake
w	Value at the wake

چکیده

در این مقاله جریان دنباله سیلندر دایروی با نصب تعدادی سیم اغتشاش‌ساز به طور تجربی مورد بررسی قرار گرفته است. هدف از این تحقیق، تعیین موقعیت بحرانی سیم نسبت به سیلندر برای قطر و عدد رینولدز خاصی می باشد که بدین منظور دنباله و گردابه های حاصل از سیلندر دایروی مورد بررسی قرار گرفته اند. همچنین موقعیت زاویه نصب سیم بر روی سیلندر مورد بررسی قرار گرفته است. قطر سیم ۱,۵ میلیمتر (نسبت قطر سیم به سیلندر ۰,۰۷۵) بوده که در موقعیت های زاویه ای مختلف (با توجه به تعداد سیم های اغتشاش ساز۲،۴،۶،۸ و ۱۰) و در دو عدد رینولدز متفاوت (به ترتیب ۱۰۰۰۰ و ۳۵۰۰۰) بر روی سیلندر قرار گرفته اند. در نتیجه با قرار دادن سیم های اغتشاش ساز در زاویه ۴۵ درجه (با تعداد ۴ سیم)، ضریب درگ با ۴۱,۶ و ۷۰,۶ درصد (به ترتیب در رینولدزهای ۱۰۰۰۰ و ۳۵۰۰۰) نسبت به سیلندر بدون سیم کاهش چشم گیری داشته است. تغییرات نموداری عدد استروهال نسبتا رابطه معکوسی با ضریب درگ نشان داده است. بیشترین، کمینه کاهش سرعت که مقداری در خط مرکزی دنباله می باشد، با بیشینه قله های شدت اغتشاشات و عرض دنباله رابطه معکوس دارد، درحالیکه با لایه برشی رابطه مستقیم دارد.

در این تحقیق برای نوآوری از تعداد ۲، ۴، ۶، ۸ و ۱۰ سیم و در دو عدد رینولدز برای نصب بر روی سیلندر استفاده شده است. همچنین در مطالعات مربوط به دیگر محققان با نصب یک و دو سیم با زاویه های ۴۵ و ۶۰ درجه بر روی سیلندر ناپایداری های زیادی مشاهده شده است که البته در این تحقیق با نصب تعداد سیم های اغتشاش ساز بیشتر در این زوایا به نتایج مطلوبی دست یافته شده است. آزمایش ها در تونل باد با سرعت پایین و دمنده دساخت شرکت فراسنجش صبا انجام شده اند. سیلندر های مورد استفاده به عنوان مدل دارای قطر ۲۰ میلیمتر و طول ۴۰۰ میلیمتر می باشند.